

Supporting Information

Preparation of $\text{Zn}_3\text{Nb}_2\text{O}_8$ anode material for high-performance lithium/sodium-ion batteries

Xuemin Yin,^{a,*} Shuling Cheng,^b Yuyang Zhang,^c Chencheng liu,^a

^aHebei Key Laboratory of Green Development of Rock and Mineral Materials, Hebei GEO University, Shijiazhuang 050031, China

^bSchool of Chemical and Environmental Engineering, Shanghai Institute of Technology, Shanghai 201418, China

^cFaculty of Robot Science and Engineering, Northeastern University, Liaoning 110819, China

*Corresponding author

E-mail: xueminyin24@163.com

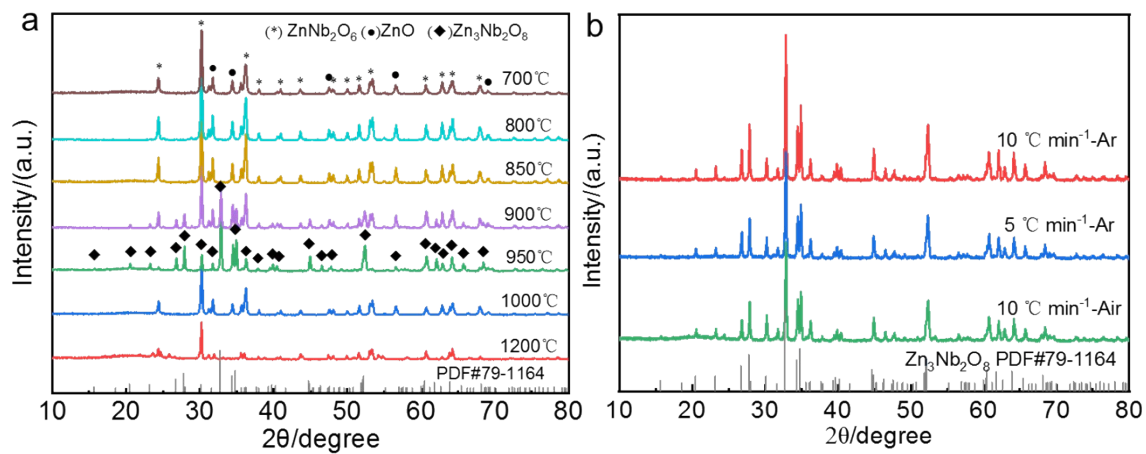


Figure S1. (a)XRD patterns of zinc niobate materials calcined to $700\text{-}1200\text{ }^{\circ}\text{C}$ at $10\text{ }^{\circ}\text{C min}^{-1}$ in air. (b)XRD patterns of zinc niobium oxide with different calcination conditions.

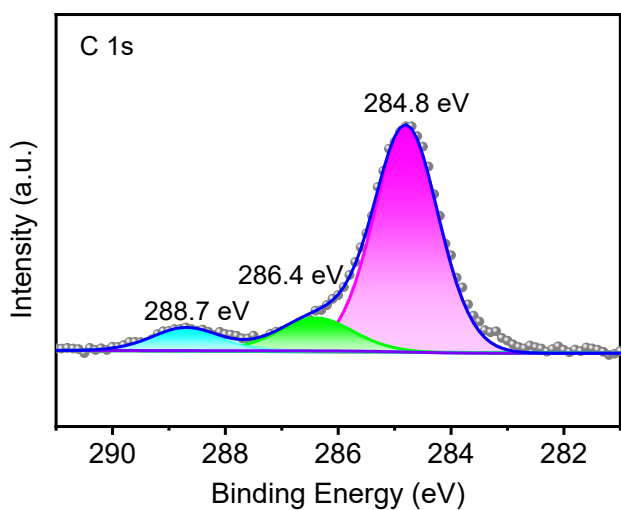


Figure S2. XPS spectra of $\text{Zn}_3\text{Nb}_2\text{O}_8$ -B for C 1s.

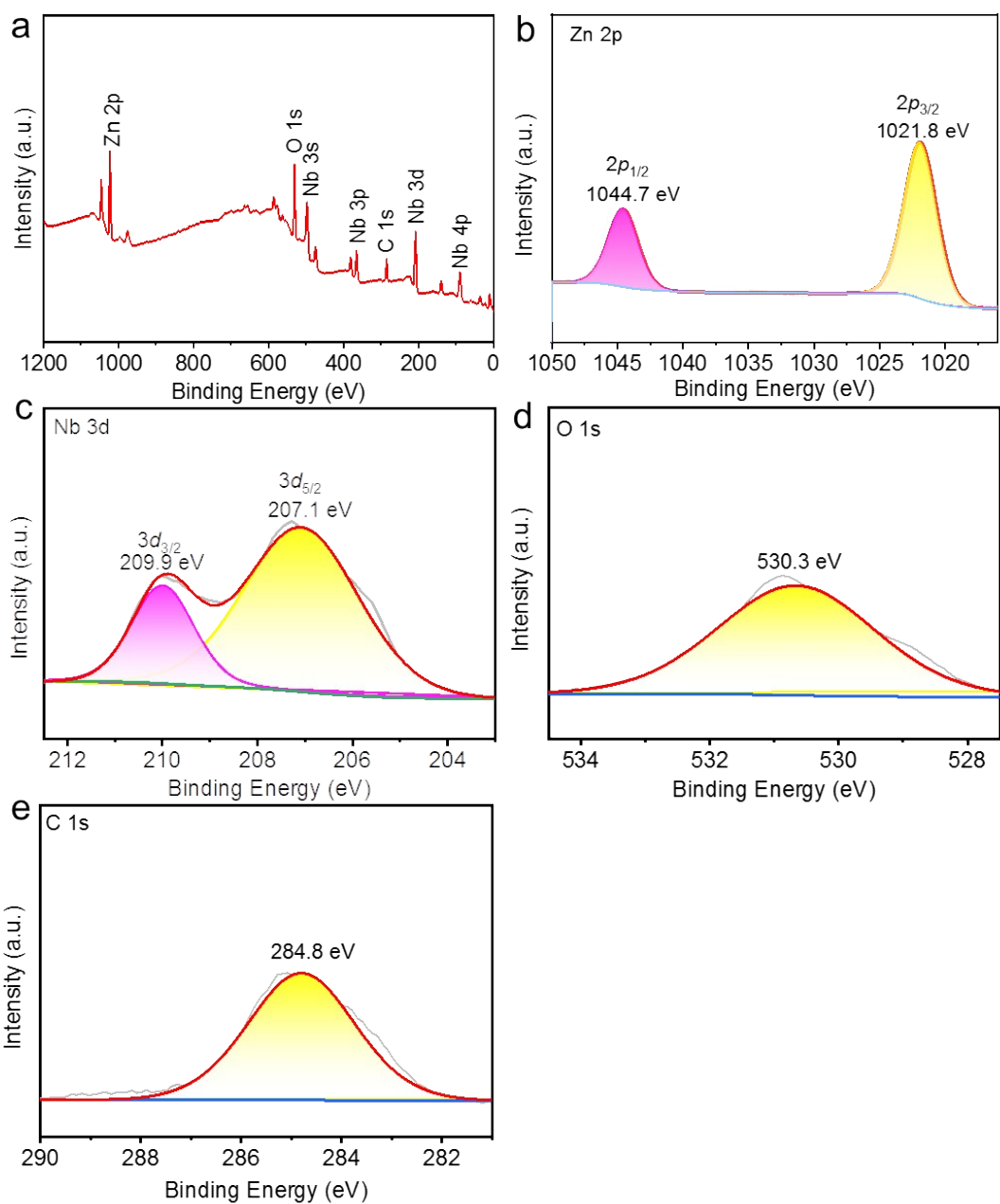


Figure S3. (a) XPS survey spectra of $\text{Zn}_3\text{Nb}_2\text{O}_8\text{-A}$; XPS spectra of $\text{Zn}_3\text{Nb}_2\text{O}_8\text{-A}$ for (b) Zn 2p, (c) Nb 3d, (d) O 1s and (e) C 1s.

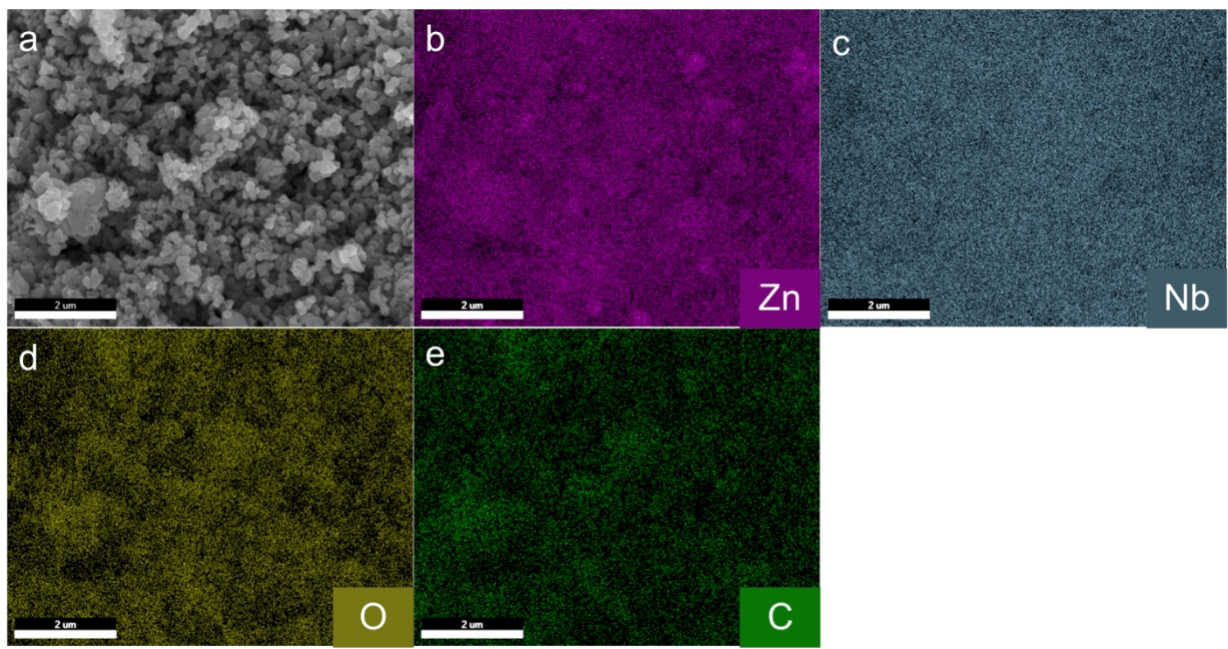


Figure S4. EDX mapping images of $\text{Zn}_3\text{Nb}_2\text{O}_8$ -A

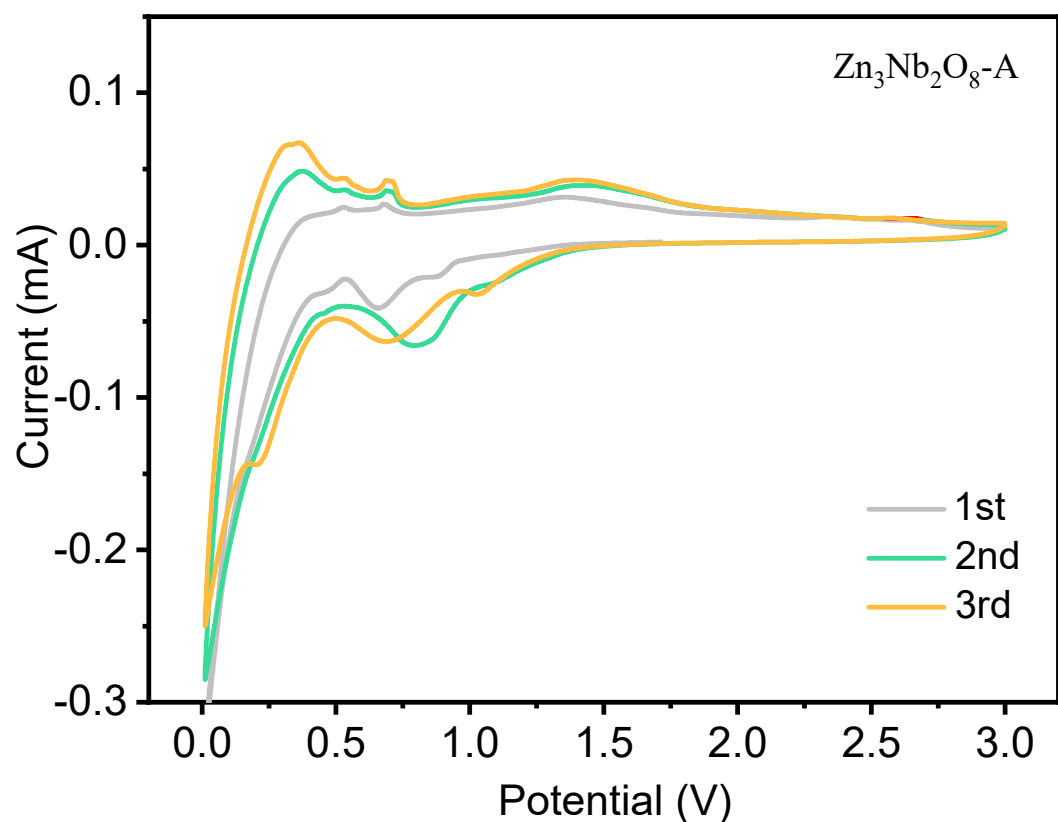


Figure S5. CV curves of $\text{Zn}_3\text{Nb}_2\text{O}_8\text{-A}$ at the scan rate of 0.1 mV s^{-1}

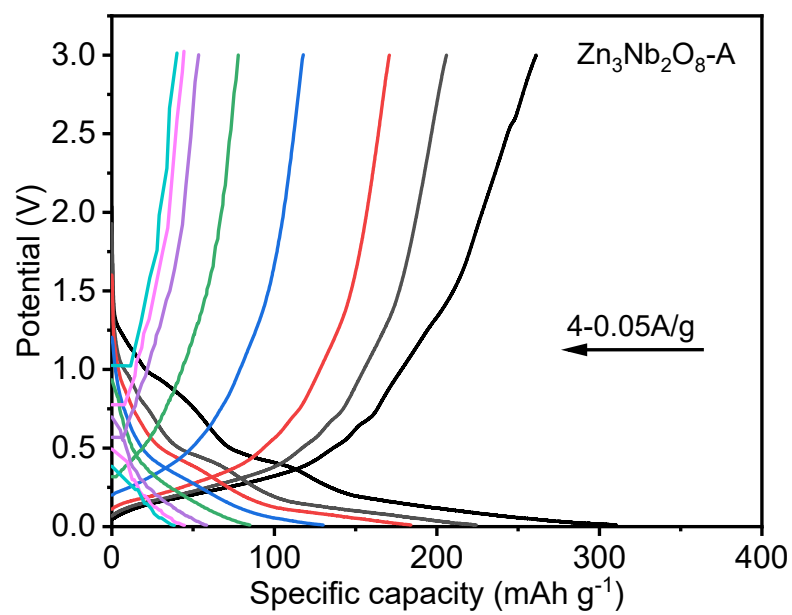


Figure S6. Galvanostatic charge/discharge (GCD) curves of $\text{Zn}_3\text{Nb}_2\text{O}_8$ -A at different current densities from 0.05 A g^{-1} to 4.0 A g^{-1}

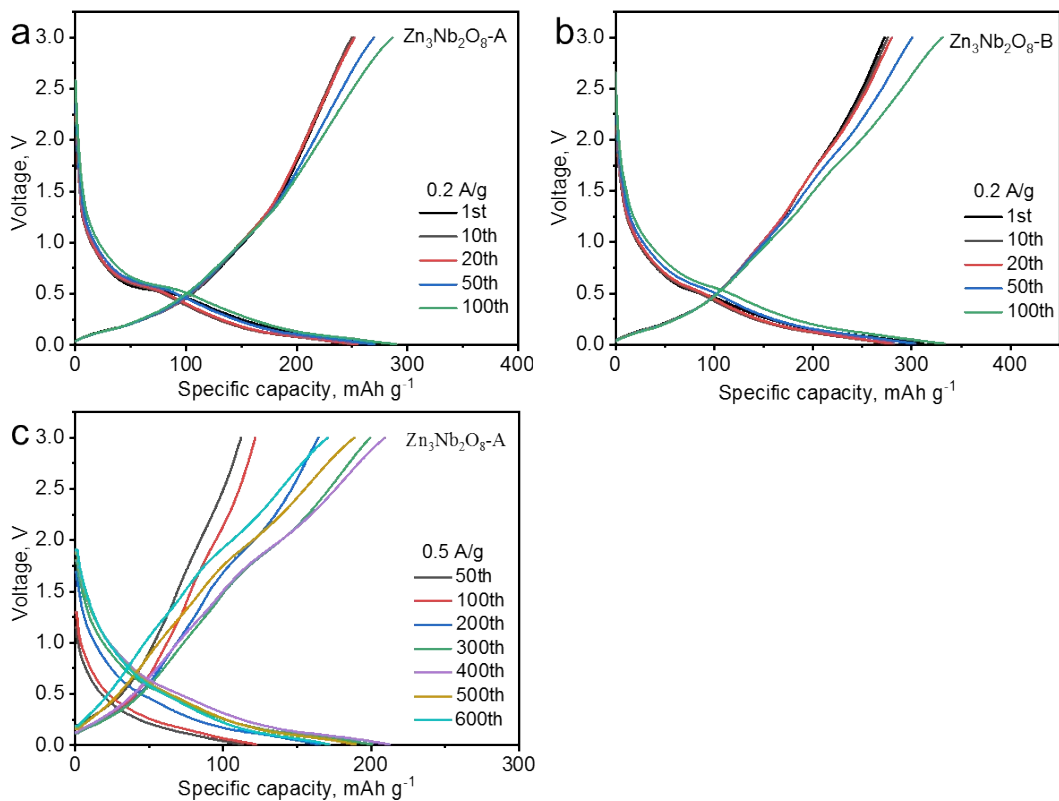


Figure S7. Discharge and charge curves of (a) $\text{Zn}_3\text{Nb}_2\text{O}_8$ -A and (b) $\text{Zn}_3\text{Nb}_2\text{O}_8$ -B at a current density of 0.2 A g^{-1} ; (c) Discharge and charge curves of $\text{Zn}_3\text{Nb}_2\text{O}_8$ -A at a current density of 0.5 A g^{-1}

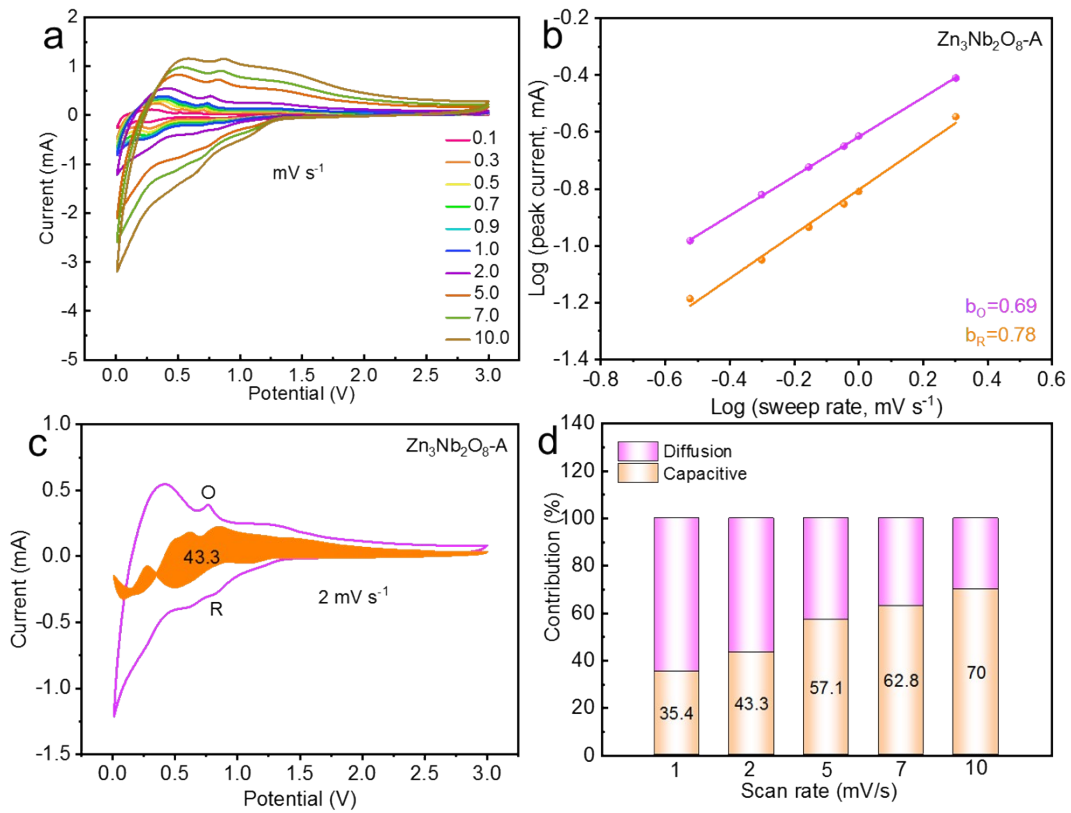


Figure S8. (a) CV curves of $\text{Zn}_3\text{Nb}_2\text{O}_8$ -A from 0.1 to 10.0 mV s^{-1} ; (b) Plots of $\log(i)$ vs. $\log(v)$ of the $\text{Zn}_3\text{Nb}_2\text{O}_8$ -A/Li cell; (c) The pseudo-capacitive contribution of $\text{Zn}_3\text{Nb}_2\text{O}_8$ -B electrode at the sweep rate of 2 mV s^{-1} ; (d) Contribution ratios of diffusion- and capacitive- controlled capacities at different scan rates.

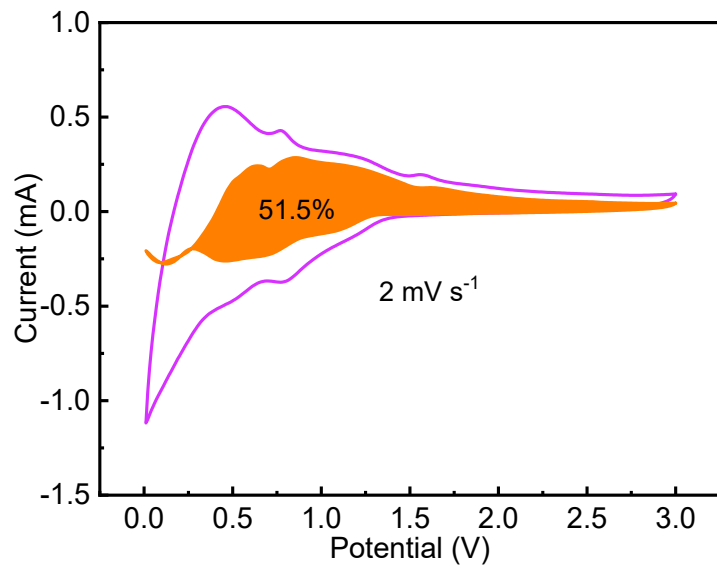


Figure S9. The pseudo-capacitive contribution of $\text{Zn}_3\text{Nb}_2\text{O}_8\text{-B}$ electrode at the sweep rate of 2 mV s^{-1} ;

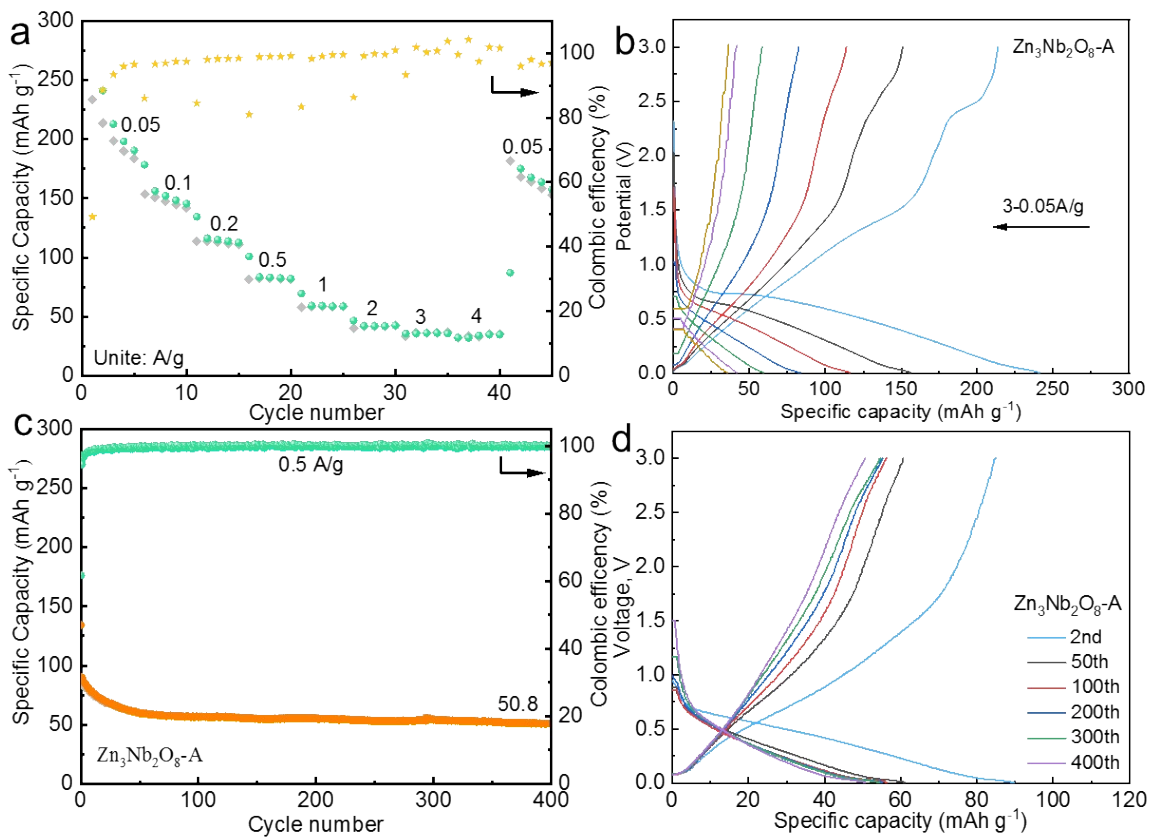


Figure S10. (a) Rate performances of $\text{Zn}_3\text{Nb}_2\text{O}_8$ -A at different current densities for SIBs; (b) Galvanostatic discharge and charge curves of $\text{Zn}_3\text{Nb}_2\text{O}_8$ -A at different current densities from 0.05 to 3.0 A g^{-1} . (c) Cycling performances of $\text{Zn}_3\text{Nb}_2\text{O}_8$ -A at a current density of 0.5 A g^{-1} ; (d) Discharge and charge curves of $\text{Zn}_3\text{Nb}_2\text{O}_8$ -A at a current density of 0.5 A g^{-1} ;

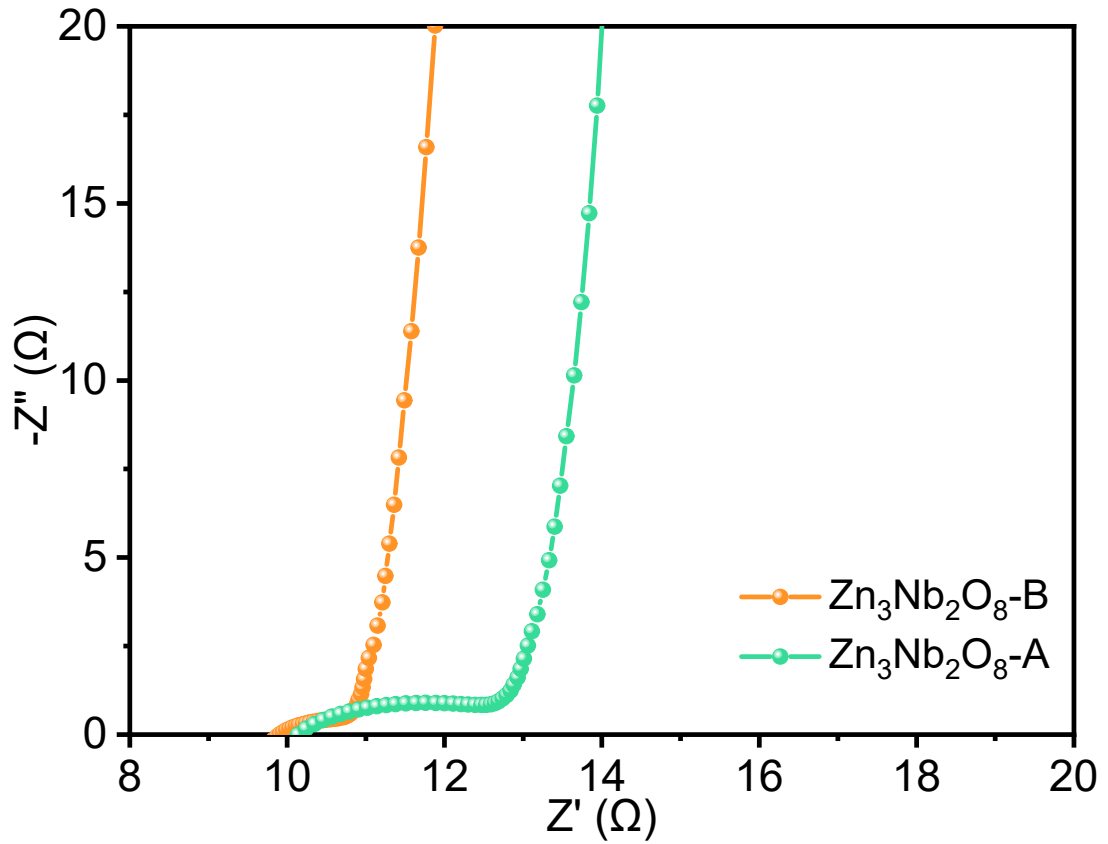


Figure S11. Nyquist plots of $Zn_3Nb_2O_8$ -A and $Zn_3Nb_2O_8$ -B

Table S1. Electrochemical energy storage performances of the reported Nb-based for the application in LIBs.

Anode	Current density (mA g ⁻¹)	Cycling stability (mAh g ⁻¹)-capacity retention	Current density (mA g ⁻¹)/ capability (mAh g ⁻¹)	Potential (V)	Ref.
Nb ₂ O ₅	50	60.0 after 100 cycles (98%)	1000/16	0.01-3.0	[1]
K ₆ Nb _{10.8} O ₃₀	100	150.0 after 400 cycles (80%)	800/50	0.5-3.0	[2]
ZnNb ₂ O ₆	100	181.9 after 100 cycles (50%)	5000/18	0.005–3.0 V	[3]
VNb ₉ O ₂₅	100	205.0 after 600 cycles (94.2%)	1000/105	1.0-3.0	[4]
Bi ₅ Nb ₃ O ₁₅	100	212.1 after 100 cycles (66.4%)	700/88.2	0.01-3.0	[5]
TiNb ₂ O ₇ @C	100	225.2 after 500 cycles (75.6%)	3880/157.9	0.01-3.0	[6]
CrNb ₄₉ O ₁₂₄	200	190.0 after 500 cycles (66%)	500/198.0	1.0-3.0	[7]
SnNb ₂ O ₆ @C	500	102.5 after 800 cycles (41%)	10000/67	0.01-3.0	[8]
GeNb ₁₈ O ₄₇	500	162.1 after 200 cycles (94.6%)	1000/123.2	1.0-3.0	[9]
WNb ₁₂ O ₃₃	700	140.0 after 700 cycles (86.1%)	700/115	1.0-3.0	[10]
Zn ₃ Nb ₂ O ₈	500	291.7 after 650 cycles (139.5%)	4000/91.4	0.01-3.0	This work

References:

- [1] G.-Y. Zeng, H. Wang, J. Guo, L.-M. Cha, Y.-H. Dou, J.-M. Ma, *Chinese Chemical Letters* **2017**, *28*, 755.
- [2] H. Zhu, X. Cheng, H. Yu, W. Ye, N. Peng, R. Zheng, T. Liu, M. Shui, J. Shu, *Nano Energy* **2018**, *52*, 192.
- [3] X.F. Li, J. Li, R.N. Ali, Z. Wang, G.J. Hu, B. Xiang, *Chemical Engineering Journal* **2019**, *368*, 764.
- [4] S. Qian, H. Yu, L. Yan, H. Zhu, X. Cheng, Y. Xie, N. Long, M. Shui, J. Shu, *ACS Applied Materials Interfaces* **2017**, *9*, 30608.
- [5] Y. Li, R. Zheng, H. Yu, X. Cheng, H. Zhu, Y. Bai, T. Liu, M. Shui, J. Shu, *Ceramics International* **2018**, *44*, 11505.
- [6] G. Zhu, Q. Li, R. Che, *Chemistry* **2018**, *24*, 12932.
- [7] W. Ye, H. Yu, X. Cheng, H. Zhu, R. Zheng, T. Liu, N. Long, M. Shui, J. Shu, *ACS Applied Energy Materials* **2019**, *2*, 2672.
- [8] T. Liu, X. Yin, X. Yin, S. Cheng, X. Wang, Y. Zhao, *Chemistry-An Asian Journal* **2022**, *17*, e202200288.
- [9] F. Ran, X. Cheng, H. Yu, R. Zheng, T. Liu, X. Li, N. Ren, M. Shui, J. Shu, *Electrochimica Acta* **2018**, *282*, 634.
- [10] L. Yan, H. Lan, H. Yu, S. Qian, X. Cheng, N. Long, R. Zhang, M. Shui, J. Shu, *Journal of Materials Chemistry A* **2017**, *5*, 8972.